COMMUNICATION

Chalcogen-Atom Abstraction Reactions of a Di-Iron Imidophosphorane Complex

Received 00th January 20xx,
Accepted 00th January 20xx

DOI: 10.1039/x0xx00000x

Luis M. Aguirre Quintana,[a] Yan Yang,[b] Arun Ramanathan,[a] Ningxin Jiang,[a] John Bacsa,[a] Laurent Maron,[b] and Henry S. La Pierre*[a,c]

Reaction of the complexes $[Fe_2(\mu_2\text{-}NP(pip)_3)_2(NP(pip)_3)_2]$ (1-Fe) and $[Co_2(\mu_2\text{-}NP(pip)_3)_2(NP(pip)_3)_2]$ (1-Co), where $[NP(pip)_3]^{1-}$ is tris(piperidinyl)imidophosphorane, with nitrous oxide, S_8, or Se^0 result in divergent reactivity. With nitrous oxide, 1-Fe forms $[Fe_2(\mu_2\text{-}O)(\mu_2\text{-}NP(pip)_3)_2(NP(pip)_3)_2]$ (2-Fe), with a very short Fe^{3+}–Fe^{3+} distance. Reactions of 1-Fe with S_8 or Se^0 results in the bridging, side-on coordination ($\mu\text{-}\kappa^1\text{:}\kappa^1\text{-}E_2^{2-}$) of the heavy chalcogens in complexes $[Fe_2(\mu\text{-}\kappa^1\text{:}\kappa^1\text{-}E_2)(\mu_2\text{-}NP(pip)_3)_2(NP(pip)_3)_2]$ (E = S, 3-Fe, or Se, 4-Fe). In all cases, the complex 1-Co is inert.

Molecular metal-metal bonded compounds are a lodestone guiding the understanding of inorganic bonding, reactivity, and magnetism.[1-4] Recently Berry, Lu, Thomas, and others have demonstrated the cooperative reactivity of bimetallic complexes in the formation of terminal metal-ligand multiple bonds via oxidative atom-transfer reactions.[5-11] In the case of iron and cobalt, most of the compounds with metal-metal bonds, beyond those supported by carbonyl ligands, form paddlewheel clusters with sterically congested ligands that inhibit any cooperative, side-on (or "facial") reactivity of the metal-metal bond. This limits the scope of atom-transfer reactions that can be accessed with diiron and dicobalt compounds. Recent examples of facial atom-transfer chemistry have been achieved with constrained geometry, strong-field, redox-active ligands.[12, 13]

An alternative approach is to employ monodentate, weak field ligands to construct reactive bimetallic complexes. Our group has recently employed tris(dialkylamido)-imidophosphoranes to expand the redox chemistry of the lanthanides and actinides.[14-18] Unlike its alkyl counterparts, the dialkylamido backbone in this ligand architecture better supports the zwitterionic character in the P–N moiety of imidophosphoranes, favoring a P^{+}–N^{2-} configuration. The pseudo-imido character results in a basic 1σ, 2π weak-field donor that is isoelectronic in its donor profile to cyclopentadienyls, or the more similar single-atom donor siloxides.[19, 20] The steric profile and donor properties of this ligand framework support low-coordinate iron and give rise to clusters with metal-metal bonds. To date, few examples exist of homoleptic iron or cobalt imidophosphorane complexes, of which, most are supported by alkyl backbones and no atom-transfer reactivity has been reported.[20-23] To this end, we set out to employ one of the tris(dialkyl)imidophosphorane variants to explore the atom-transfer chemistry between well-defined homoleptic Fe(II) and Co(II) complexes and N_2O, S_8, and Se^0.

The reaction of two equivalents of $FeCl_2$ or $CoCl_2$ with four equivalents of $K[NP(pip)_3]$ in THF[16] results in the isolation of the bimetallic complexes $[Fe_2(\mu_2\text{-}NP(pip)_3)_2(NP(pip)_3)_2]$ (**1-Fe**) and $[Co_2(\mu_2\text{-}NP(pip)_3)_2(NP(pip)_3)_2]$ (**1-Co**) in 79% and 73% yield, respectively. Complex **1-Fe** crystalizes in the $P\bar{1}$ space group with two molecules in the asymmetric unit. Single-crystal XRD (SC-XRD) analysis of **1-Fe** reveals the molecular structure shown in Figure 1. The product is a saddled Fe_2^{4+} bimetallic complex with two μ–$[NP(pip)_3]^{-}$ ligands bridging each Fe^{2+} center and a terminal $[NP(pip)_3]^{-}$ ligand at each metal center. The average Fe–Fe distance in **1-Fe** is 2.6141(6) Å, which falls within the range of a metal-metal bond[24, 25] with a formal-shortness ratio

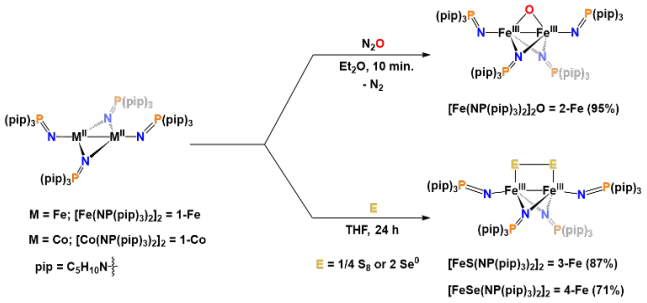

Scheme 1. Synthesis of **2-Fe**.

[a] Department of Chemistry and Biochemistry, Georgia Institute of Technology, Atlanta, Georgia 30332-0400, USA. E-mail: hsl@gatech.edu
[b] Laboratorie de Physique et Chimie des Nano-objects, Institute National Des Sciences Appliquees, 31077 Toulouse, Cedex 4, France.
[c] Nuclear and Radiological Engineering Program, Georgia Institute of Technology, Atlanta, Georgia 30332-0400, USA.

† Electronic supplementary information (ESI) available: Experimental procedures and crystallographic data (PDF and CIF). CCDC 2077656, 2077657, 2077658, 2077659, and 2078817. For ESI and crystallographic data in CIF or other electronic format see DOI: XXXXXXXXXXXXXXXXXX

(FSR) of 1.05. Crystallographically, **1-Co** is isomorphic and isostructural to **1-Fe** (See ESI).

The $[NP(pip)_3]^-$ ligand supports low-coordinate Fe^{2+} and Co^{2+} compounds with facially exposed metal-metal bonds. The reactivity of these dimetallic complexes was examined with chalcogen-atom transfer reagents: N_2O, S, and Se^0. Exposure of a solution of **1-Fe** or **1-Co** to an atmosphere of N_2O led to a reaction in 10 minutes for **1-Fe**. The resulting brown product, $[Fe_2(\mu_2\text{-}O)(\mu_2\text{-}NP(pip)_3)_2(NP(pip)_3)_2]$, (**2-Fe**), was isolated in 95 % yield. Under the same conditions, **1-Co** showed no reactivity with N_2O. The molecular structure of **2-Fe** is shown in Figure 1 and crystalizes in the $P\bar{1}$ space group. Similar to **1-Fe**, the structure of **2-Fe** reveals a bimetallic complex with two μ–$[NP(pip)_3]^-$ ligands bridging the Fe^{3+} centers and a terminal $[NP(pip)_3]^-$ligand at each metal center. Additionally, the metal centers are bridged by a $\mu\text{–}O^{2-}$ ligand. The average terminal Fe–N_{imido} distance in **2-Fe** is 1.8372(12) Å and the average bridging Fe–N_{imido} distance is 2.0265(2) Å, which shows elongation in Fe–N_{imido} distances in comparison to **1-Fe**. The average terminal and bridging P–N_{imido} distances in **2-Fe** are 1.5395(2) Å and 1.5475(2) Å, respectively, similar to those in **1-Fe**. Notably, the distance between the Fe(III) centers in **2-Fe** is 2.3396(6) Å, and is one of the shortest Fe–Fe distances, which typically involve Fe_2^{2+}, Fe_2^{3+}, Fe_2^{4+}, and Fe_2^{5+} cores.[24] There are no other examples of dinuclear complexes with an Fe_2^{6+} core with metal centers within the metric range for an Fe^{3+}–Fe^{3+} bond. The Fe–Fe distance in **2-Fe** is in fact shorter than that of a reported single bond distance (248 pm),[26] giving it a formal shortness ratio (FSR) of 0.94. Whether this distance is the consequence of a metal–metal bond or the geometric constraint of the bridging O^{2-} is under further investigation.

Nitrous oxide is a greenhouse gas and its potential utilization as a green oxidant has become an important technological target.[27] It is a thermodynamically potent oxidant, but kinetically poor.[27-29] To date, few examples of molecular iron and cobalt compounds have been reported to bind or activate N_2O under mild conditions and stable, oxidized complexes are rare.[30-33] Therefore, the reactivity between **1-Fe** and N_2O is noteworthy since it produces an isolable oxygen-atom abstraction product that does not undergo further intramolecular reaction with ligand C–H bonds. To gain insight into the observed reactivity, an energy profile for the reaction between **1-Fe** and N_2O was calculated at the DFT level (B3PW91) as shown in Figure 2. The energy profile reveals initial binding of N_2O in the κ_1-O mode to one of the Fe(II) centers in **1-Fe** (a κ_2-N,O binding event was not found on the intrinsic reaction coordinate). This unsymmetrical coordination is exothermic by 2.1 kcal.mol^{-1}. From this adduct, the system evolves to a N–O bond breaking transition state. The N–O bond breaking is favoured by the nucleophilic assistance of the second iron center (Fe–O distance of 1.99 and 2.53 Å). The associated barrier is 4.1 kcal.mol^{-1} from the adduct (2.0 kcal.mol^{-1} from the entrance channel), which is much lower than that calculated for other systems.[34, 35] Following the intrinsic reaction coordinate, it yields complex **2-Fe** whose formation is thermodynamically favoured with the production and release of N_2 gas. This reaction profile indicates that the

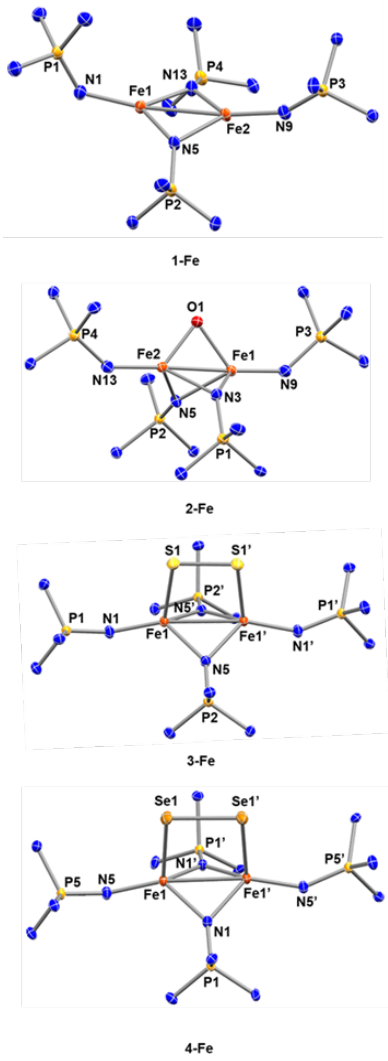

Figure 1. Molecular structures of **1-Fe**, **2-Fe**, **3-Fe**, and **4-Fe** shown with thermal ellipsoids at 50% probability. Piperidinyl carbon and hydrogen atoms are omitted for clarity. Only one of the two molecules in the asymmetric unit of **1-Fe** is shown here. See ESI for full structures.

metal-metal bonded iron centers in **1-Fe** are able to participate synergistically to carry out the two-electron reduction of N_2O by undergoing a one-electron oxidation at each metal center.

To further assess the reactivity of **1-Fe** and **1-Co** with other chalcogen-atom transfer reagents their reactions with elemental sulfur (S_8) and selenium metal powder (Se^0) were examined. In both cases, **1-Fe** or **1-Co** were dissolved in THF and added to a stirring suspension of S_8 or Se^0. After isolation, $[Fe_2(\mu\text{-}\kappa^1\text{:}\kappa^1\text{-}S_2)(\mu_2\text{-}NP(pip)_3)_2(NP(pip)_3)_2]$ (**3-Fe**) and $[Fe_2(\mu\text{-}\kappa^1\text{:}\kappa^1\text{-}Se_2)(\mu_2\text{-}NP(pip)_3)_2(NP(pip)_3)_2]$ (**4-Fe**) were recovered in 87 % and 71 %, respectively (Scheme 1). As with the reaction with N_2O, no reaction was observed between **1-Co** and S_8 or Se^0. Compounds **3-Fe** and **4-Fe** both crystallize in the *C2/c* space group and are crystallographic dimers comprised of two μ–$[NP(pip)_3]^-$ ligands bridging each Fe^{3+} center and a terminal $[NP(pip)_3]^-$ ligands at each metal center. The metal centers in **3-Fe** and **4-Fe** are bridged by a $(\mu\text{-}\kappa^1\text{:}\kappa^1\text{-}S_2)^{2-}$ and $(\mu\text{-}\kappa^1\text{:}\kappa^1\text{-}Se_2)^{2-}$ ligand, respectively, which sits above and parallel to the to the

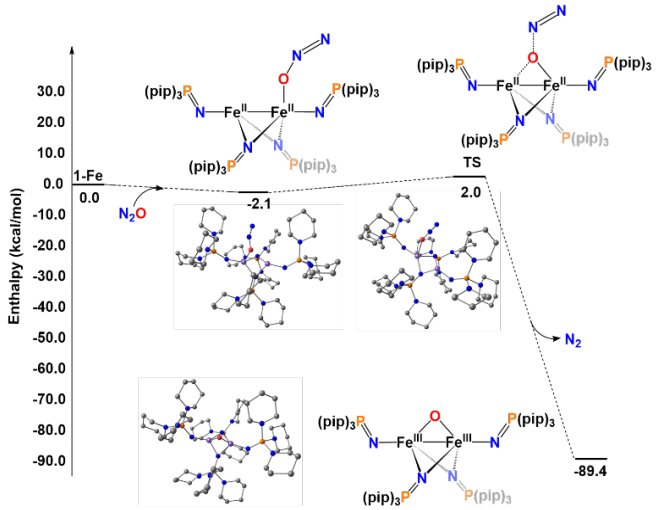

Figure 2. Computed enthalpy profile at room temperature for the reaction of **1-Fe** with N_2O.

Fe–Fe axis in both compounds as shown in Figure 1. The average Fe–E and E–E distances in **3-Fe** and **4-Fe** (where E = S or Se, respectively) are 2.3258(4) and 2.0847(6) Å and 2.4582(8) and 2.3532(8) Å which are consistent with in other reported iron-sulfido and -selenido compounds.[36-38] The Fe–Fe distances in **3-Fe** and **4-Fe** are 2.5964(6) and 2.6072(6) Å which are longer than **2-Fe**, but have an FSR of 1.05 for both complexes, similar to that of **1-Fe** in the Fe_2^{6+} core.[24]

The "side-on" binding of the $(\mu\text{-}\kappa^1\text{:}\kappa^1\text{-}S_2)^{2-}$ and $(\mu\text{-}\kappa^1\text{:}\kappa^1\text{-}Se_2)^{2-}$ ligands is unique with E–E bind above and parallel to the Fe–Fe axis in **3-Fe** and **4-Fe**.[38-41] Iron–sulfido cluster compounds are commonly produced oxidation products from the reduction of elemental sulfur and are bridged by a S^{2-} ligand.[42] Diiron compounds supported by a S_2^{2-} ligand are rarer and often bridged by a S_2^{2-} that is oblique and/or perpendicular to the Fe–Fe axis.[43] Of the few examples of non-carbonyl iron selenido molecular compounds, only one diiron compound presents a similar bridging $(\mu\text{-}\kappa^1\text{:}\kappa^1\text{-}Se_2)^{2-}$ ligand. [44, 45]

In conclusion, we have reported the synthesis of the homoleptic bimetallic Fe^{2+} and Co^{2+} compounds **1-Fe** and **1-Co** supported by the $[NP(pip)_3]^-$ ligand, which featured low-coordinate metal-metal bonds with readily accessible synergistic, facial reactivity in the case of **1-Fe**. Compound **1-Fe** displayed unique chalcogen-atom abstraction reactivity with N_2O, S_8, and Se^0 to produce compounds **2-Fe**, **3-Fe**, **4-Fe**. Structural analysis revealed that **2-Fe** has one of the shortest Fe-Fe distances observed in a diiron compound unsupported by carbonyl or guanidinate ligands and that **3-Fe** and **4-Fe** produce bimetallic compounds with an Fe_2^{6+} core and fairly short intermetallic distances, where the Fe(III) centers are bridged by $(\mu\text{-}\kappa^1\text{:}\kappa^1\text{-}S_2)^{2-}$ and $(\mu\text{-}\kappa^1\text{:}\kappa^1\text{-}Se_2)^{2-}$ ligands parallel to the metal-metal axis. The electronic structure driving the unique and divergent reactivity of **1-Fe** and the structures of **2-Fe**, **3-Fe**, and **4-Fe** will be reported soon.

Conflicts of interest

There are no conflicts to declare.

Acknowledgements

This work was supported by NSF grant CHE-1943452 and a CONACYT Graduate Fellowship to LMAQ. LM is a senior member of the Institut Universitaire de France. The Chinese Scholarship Council and the Chinese Academy of Science are acknowledged for financial support and CalMip for a generous grant of computing time.

References

1. J. F. Berry and C. C. Lu, Metal–Metal Bonds: From Fundamentals to Applications, *Inorg. Chem.*, 2017, **56**, 7577-7581.
2. F. A. Cotton, N. F. Curtis, C. B. Harris, B. F. G. Johnson, S. J. Lippard, J. T. Mague, W. R. Robinson and J. S. Wood, Mononuclear and Polynuclear Chemistry of Rhenium (III): Its Pronounced Homophilicity, *Science*, 1964, **145**, 1305.
3. T. Nguyen, A. D. Sutton, M. Brynda, J. C. Fettinger, G. J. Long and P. P. Power, Synthesis of a Stable Compound with Fivefold Bonding Between Two Chromium(I) Centers, *Science*, 2005, **310**, 844.
4. J. E. McGrady, in *Molecular Metal-Metal Bonds*, ed. S. T. Liddle, Wiley, 2015, ch. 1, pp. 1-22.
5. K. P. Kornecki, J. F. Briones, V. Boyarskikh, F. Fullilove, J. Autschbach, K. E. Schrote, K. M. Lancaster, H. M. L. Davies and J. F. Berry, Direct Spectroscopic Characterization of a Transitory Dirhodium Donor-Acceptor Carbene Complex, *Science*, 2013, **342**, 351.
6. J. R. Prat, C. A. Gaggioli, R. C. Cammarota, E. Bill, L. Gagliardi and C. C. Lu, Bioinspired Nickel Complexes Supported by an Iron Metalloligand, *Inorg. Chem.*, 2020, **59**, 14251-14262.
7. R. C. Cammarota, M. V. Vollmer, J. Xie, J. Ye, J. C. Linehan, S. A. Burgess, A. M. Appel, L. Gagliardi and C. C. Lu, A Bimetallic Nickel–Gallium Complex Catalyzes CO_2 Hydrogenation via the Intermediacy of an Anionic d^{10} Nickel Hydride, *J. Am. Chem. Soc.*, 2017, **139**, 14244-14250.
8. B. Wu, M. J. T. Wilding, S. Kuppuswamy, M. W. Bezpalko, B. M. Foxman and C. M. Thomas, Exploring Trends in Metal–Metal Bonding, Spectroscopic Properties, and Conformational Flexibility in a Series of Heterobimetallic Ti/M and V/M Complexes (M = Fe, Co, Ni, and Cu), *Inorg. Chem.*, 2016, **55**, 12137-12148.
9. J. Coombs, D. Perry, D.-H. Kwon, C. M. Thomas and D. H. Ess, Why Two Metals Are Better Than One for Heterodinuclear Cobalt–Zirconium-Catalyzed Kumada Coupling, *Organometallics*, 2018, **37**, 4195-4203.
10. J. P. Krogman, M. W. Bezpalko, B. M. Foxman and C. M. Thomas, Multi-electron redox processes at a Zr(IV) center facilitated by an appended redox-active cobalt-containing metalloligand, *Dalton Trans.*, 2016, **45**, 11182-11190.
11. J. P. Krogman, B. M. Foxman and C. M. Thomas, Formation and Subsequent Reactivity of a N_2-Stabilized Cobalt–Hydride Complex, *Organometallics*, 2015, **34**, 3159-3166.
12. Y.-Y. Zhou, D. R. Hartline, T. J. Steiman, P. E. Fanwick and C. Uyeda, Dinuclear Nickel Complexes in Five States of Oxidation Using a Redox-Active Ligand, *Inorg. Chem.*, 2014, **53**, 11770-11777.

13. S. Zhang, P. Cui, T. Liu, Q. Wang, T. J. Longo, L. M. Thierer, B. C. Manor, M. R. Gau, P. J. Carroll, G. C. Papaefthymiou and N. C. Tomson, N−H Bond Formation at a Diiron Bridging Nitride, *Angew. Chem. Int. Ed.*, 2020, **59**, 15215-15219.
14. T. P. Gompa, A. Ramanathan, N. T. Rice and H. S. La Pierre, The chemical and physical properties of tetravalent lanthanides: Pr, Nd, Tb, and Dy, *Dalton Trans.*, 2020, **49**, 15945-15987.
15. N. T. Rice, K. McCabe, J. Bacsa, L. Maron and H. S. La Pierre, Two-Electron Oxidative Atom Transfer at a Homoleptic, Tetravalent Uranium Complex, *J. Am. Chem. Soc.*, 2020, **142**, 7368-7373.
16. N. T. Rice, J. Su, T. P. Gompa, D. R. Russo, J. Telser, L. Palatinus, J. Bacsa, P. Yang, E. R. Batista and H. S. La Pierre, Homoleptic Imidophosphorane Stabilization of Tetravalent Cerium, *Inorg. Chem.*, 2019, **58**, 5289-5304.
17. N. T. Rice, I. A. Popov, D. R. Russo, J. Bacsa, E. R. Batista, P. Yang, J. Telser and H. S. La Pierre, Design, Isolation, and Spectroscopic Analysis of a Tetravalent Terbium Complex, *J. Am. Chem. Soc.*, 2019, **141**, 13222-13233.
18. N. T. Rice, I. A. Popov, D. R. Russo, T. P. Gompa, A. Ramanathan, J. Bacsa, E. R. Batista, P. Yang and H. S. La Pierre, Comparison of tetravalent cerium and terbium ions in a conserved, homoleptic imidophosphorane ligand field, *Chem. Sci.*, 2020, **11**, 6149-6159.
19. A. Sundermann and W. W. Schoeller, Phosphorane−Iminato Complexes of Transition Metals with Heterocubane Structure: A Computational Study, *J. Am. Chem. Soc.*, 2000, **122**, 4729-4734.
20. K. Dehnicke, M. Krieger and W. Massa, Phosphoraneiminato complexes of transition metals, *Coord. Chem. Rev.*, 1999, **182**, 19-65.
21. J. Camacho-Bunquin, M. J. Ferguson and J. M. Stryker, Hydrocarbon-Soluble Nanocatalysts with No Bulk Phase: Coplanar, Two-Coordinate Arrays of the Base Metals, *J. Am. Chem. Soc.*, 2013, **135**, 5537-5540.
22. K. Chakarawet, P. C. Bunting and J. R. Long, Large Anisotropy Barrier in a Tetranuclear Single-Molecule Magnet Featuring Low-Coordinate Cobalt Centers, *J. Am. Chem. Soc.*, 2018, **140**, 2058-2061.
23. K. Chakarawet, M. Atanasov, J. Marbey, P. C. Bunting, F. Neese, S. Hill and J. R. Long, Strong Electronic and Magnetic Coupling in M_4 (M = Ni, Cu) Clusters via Direct Orbital Interactions between Low-Coordinate Metal Centers, *J. Am. Chem. Soc.*, 2020, **142**, 19161-19169.
24. S. J. Tereniak and C. C. Lu, in *Molecular Metal-Metal Bonds*, ed. S. T. Liddle, Wiley, 2015, ch. 8, pp. 225-278.
25. C. A. Murillo, An Iron Complex with an Unsupported Fe–Fe Bond, *Angew. Chem. Int. Ed.*, 2009, **48**, 5076-5077.
26. L. Pauling, Metal-metal bond lengths in complexes of transition metals, *Proceedings of the National Academy of Sciences*, 1976, **73**, 4290.
27. M. Konsolakis, Recent Advances on Nitrous Oxide (N_2O) Decomposition over Non-Noble-Metal Oxide Catalysts: Catalytic Performance, Mechanistic Considerations, and Surface Chemistry Aspects, *ACS Catalysis*, 2015, **5**, 6397-6421.
28. A. K. Uriarte, M. A. Rodkin, M. J. Gross, A. S. Kharitonov and G. I. Panov, in *Studies in Surface Science and Catalysis*, eds. R. K. Grasselli, S. T. Oyama, A. M. Gaffney and J. E. Lyons, Elsevier, 1997, vol. 110, pp. 857-864.
29. W. B. Tolman, Binding and Activation of N_2O at Transition-Metal Centers: Recent Mechanistic Insights, *Angew. Chem. Int. Ed.*, 2010, **49**, 1018-1024.
30. K. Severin, Synthetic chemistry with nitrous oxide, *Chem. Soc. Rev.*, 2015, **44**, 6375-6386.
31. S. Yang, W. Zhu, Q. Zhang and Y. Wang, Iron-catalyzed propylene epoxidation by nitrous oxide: Effect of boron on structure and catalytic behavior of alkali metal ion-modified FeOx/SBA-15, *Journal of Catalysis*, 2008, **254**, 251-262.
32. G. Kiefer, L. Jeanbourquin and K. Severin, Oxidative Coupling Reactions of Grignard Reagents with Nitrous Oxide, *Angew. Chem. Int. Ed.*, 2013, **52**, 6302-6305.
33. W. H. Harman and C. J. Chang, N_2O Activation and Oxidation Reactivity from a Non-Heme Iron Pyrrole Platform, *J. Am. Chem. Soc.*, 2007, **129**, 15128-15129.
34. A. Delabie, C. Vinckier, M. Flock and K. Pierloot, Evaluating the Activation Barriers for Transition Metal N_2O Reactions, *The Journal of Physical Chemistry A*, 2001, **105**, 5479-5485.
35. L. Zhao, Y. Wang, W. Guo, H. Shan, X. Lu and T. Yang, Theoretical Investigation of the Fe^+-Catalyzed Oxidation of Acetylene by N_2O, *The Journal of Physical Chemistry A*, 2008, **112**, 5676-5683.
36. L. Zhou, G. Li, Q.-S. Li, Y. Xie and R. B. King, The diversity of iron−sulfur bonding in binuclear iron carbonyl sulfides, *Canadian Journal of Chemistry*, 2014, **92**, 750-757.
37. P. Mathur, R. S. Ji, A. Raghuvanshi, M. Tauqeer and S. M. Mobin, Cleavage of phosphorus-sulfur bond and formation of $(\mu_4\text{-S})Fe_4$ core from photochemical reactions of $Fe(CO)_5$ with $[(RO)_2PS_2]_2$; (R = Me, Et, iPr), *J. Organomet. Chem.*, 2017, **835**, 31-38.
38. R. S. Laitinen and R. Oilunkaniemi, in *Reference Module in Chemistry, Molecular Sciences and Chemical Engineering*, Elsevier, 2019, pp. 1-50.
39. M. Akita, in *Comprehensive Organometallic Chemistry III*, eds. D. M. P. Mingos and R. H. Crabtree, Elsevier, Oxford, 2007, pp. 259-292.
40. A. Müller and E. Diemann, in *Advances in Inorganic Chemistry*, eds. H. J. Emeléus and A. G. Sharpe, Academic Press, 1987, vol. 31, pp. 89-122.
41. M. Shieh, C.-Y. Miu, Y.-Y. Chu and C.-N. Lin, Recent progress in the chemistry of anionic groups 6–8 carbonyl chalcogenide clusters, *Coord. Chem. Rev.*, 2012, **256**, 637-694.
42. H. Ogino, S. Inomata and H. Tobita, Abiological Iron−Sulfur Clusters, *Chem. Rev.*, 1998, **98**, 2093-2122.
43. T. Mitsui, S. Inomata and H. Ogino, Syntheses of closo-$Cp'_2(CO)_3Fe_2MS_2$ Clusters (Cp' = η_5-C_5Me_5; M = Fe, Ru) and Molecular Structure of $Cp'_2(CO)_3Fe_3S_2$, *Inorg. Chem.*, 1994, **33**, 4934-4936.
44. L. C. Roof and J. W. Kolis, New developments in the coordination chemistry of inorganic selenide and telluride ligands, *Chem. Rev.*, 1993, **93**, 1037-1080.
45. M. Reiners, M. Maekawa, C. G. Daniliuc, M. Freytag, P. G. Jones, P. S. White, J. Hohenberger, J. Sutter, K. Meyer, L. Maron and M. D. Walter, Reactivity studies on [Cp'Fe(μ-I)]2: nitrido-, sulfido- and diselenide iron complexes derived from pseudohalide activation, *Chem. Sci.*, 2017, **8**, 4108-4122.

